European Polymer Journal 46 (2010) 984–996

Contents lists available at ScienceDirect

European Polymer Journal

journal homepage: www.elsevier.com/locate/europolj

MACROMOLECULAR NANOTECHNOLOGY

Macromolecular Nanotechnology

Qualitative assessment of nanofiller dispersion in poly(ε-caprolactone) nanocomposites by mechanical testing, dynamic rheometry and advanced thermal analysis

Hans E. Miltner [a], Nick Watzeels [a], Christophe Block [a], Nicolaas-Alexander Gotzen [a], Guy Van Assche [a], Koen Borghs [b], Kurt Van Durme [b], Bruno Van Mele [a], Bogdan Bogdanov [b], Hubert Rahier [a,*]

[a] Vrije Universiteit Brussel (VUB), Physical Chemistry and Polymer Science (FYSC), Pleinlaan 2, B-1050 Brussels, Belgium
[b] Orfit Industries n.v., Vosveld 9a, B-2110 Wijnegem, Belgium

ARTICLE INFO

Article history:
Received 17 June 2009
Received in revised form 26 December 2009
Accepted 9 January 2010
Available online 15 January 2010

Keywords:
Poly(ε-caprolactone) PCL
Nanocomposite
Dispersion
Silicate clay
Carbon nanotube

ABSTRACT

A comprehensive overview of available methods for assessing nanofiller dispersion is presented for a wide range of layered silicate-based poly(ε-caprolactone) (PCL) nanocomposites. Focusing on their respective strengths and weaknesses, rheological, mechanical and thermal characterization approaches are evaluated in direct relation to morphological information. Pronounced changes in the rheological and mechanical properties of the materials are only observed for nanocomposites displaying the highest nanofiller dispersion levels, as confirmed by an innovative and highly reliable thermal analysis approach based on quasi-isothermal crystallization. As such, the data obtained from the different methods also allow a detailed investigation of the crucial factors affecting nanofiller dispersion, evidencing the importance of specific matrix/filler interactions and the need for proper melt processing conditions when targeting significant property enhancements. Finally, the wide potential of the developed methodologies for the characterization of polymeric nanocomposites in general is illustrated by an extension to carbon nanotube-based PCL composites, unambiguously demonstrating their complementarity and broad applicability.

1. Introduction

It is well-established that the considerable property improvements achieved upon incorporation of nano-sized fillers into a polymeric matrix can be attributed to the extremely small size and high aspect ratio of the reinforcement, generating a tremendous amount of matrix/filler interface available for interfacial interaction. As a result, virtually the entire matrix polymer in a nanocomposite is located in close vicinity of the filler particles, effectively forming an *interphase* with strongly altered properties. A prerequisite for the latter, however, is the achievement of high levels of nanofiller dispersion in order to benefit from the high specific surface area provided by the reinforcing particles. Proper stress transfer and the targeted establishment of superior mechanical properties – amongst others – are therefore intimately related to the critical issues governing the achievable nanofiller dispersion state, i.e., a sufficient affinity between polymer and filler through the occurrence of specific interactions, along with well-adjusted melt processing conditions.

It is to be noted that the term "nanofiller dispersion" – in the context of the present paper – refers to the extent of nanofiller *individualization* throughout the polymeric matrix. Polymer nanocomposites usually form complex structures, often consisting of a mixture of different

* Corresponding author. Address: Vrije Universiteit Brussel (VUB), Faculty of Engineering, Physical Chemistry and Polymer Science (FYSC), Pleinlaan 2, B-1050 Brussels, Belgium. Tel.: +32 (0)2 629 32 77; fax: +32 (0)2 629 32 78.
E-mail address: hrahier@vub.ac.be (H. Rahier).

0014-3057/$ - see front matter © 2010 Elsevier Ltd. All rights reserved.
doi:10.1016/j.eurpolymj.2010.01.002

morphologies, the relative amount of which determines the final material properties. In layered silicate nanocomposites, original particles (micron-size aggregates) are generally broken up into tactoids (stacks of several silicate layers) and preferably further disintegrated into individual silicate layers, which depending on loading level and platelet orientation tend to form a network of silicate platelets throughout the polymeric matrix. In carbon nanotube composites, a morphology is generally aimed for in which bundles of entangled nanoparticles are disaggregated into individual carbon nanotubes, spatially distributed to generate a network of interconnected tubes throughout the material. When discussing nanocomposites in terms of dispersion quality, it is therefore a generally accepted view that "achieving a high degree of nanofiller dispersion" refers to achieving a high degree of platelet exfoliation in the context of layered silicate nanocomposites, while it indicates the extent to which tubes occur individually, hence disaggregated and unbundled, in the context of carbon nanotube composites.

There have been numerous attempts to estimate the extent of nanofiller dispersion by qualitative or semi-quantitative approaches, e.g., through the use of the shear thinning exponent from steady-shear rheometry [1], through the detailed examination of silicate network formation in dynamic rheometry experiments [2], or through the extraction of an average particle aspect ratio from either gas permeation data using numerical predictions [3] or from mechanical properties by applying the classical composite theories of Mori–Tanaka and Halpin–Tsai [4], to mention just a few. Notwithstanding the merits of these approaches, they do not allow to address the morphological hierarchy of nanocomposites at different length scales [5]. For polymer nanocomposite material design to be truly successful, the continued development of reliable methods for characterizing the nanofiller dispersion therefore appears as a crucial need.

It is the aim of the present paper to discuss the benefits and limitations of several methods available for evaluating nanofiller dispersion, as applied to poly(ε-caprolactone) nanocomposites containing layered silicates. Poly(ε-caprolactone) (PCL) is a semi-crystalline biodegradable aliphatic polyester that, owing to its fair mechanical performance, good processability, and high degree of biocompatibility [6], finds potential application in environmentally benign packaging materials, and has found widespread use in a number of biomedical applications, both *in vivo* (tissue engineering, controlled drug release) [7] as well as for external use (e.g., various medical devices) [8].

So far, however, the large-scale introduction of PCL as a 'green' alternative to various widely used polymers was hampered by some of its intrinsic weaknesses, especially in those application fields imposing rather demanding requirements to the material in terms of stiffness. Preparation of PCL nanocomposites by incorporation of low amounts of nano-sized filler particles may provide an effective way to meet those high standards [9–13]. The presence of 3–5 wt.% of layered silicates was reported to significantly increase the modulus of the PCL matrix material, while retaining its good processability and recyclability [14–16]. Moreover, incorporation of layered clay minerals strongly reduces the permeation of solvents and gases with respect to unfilled PCL [14]. Small amounts of carbon nanotubes are known to provide mechanical reinforcement as well as to generate both thermal and electrical conductivity [17–20]. In addition, a strong nucleating effect on the crystallization of PCL has been reported [17,18], imparting enhanced dimensional stability and allowing a significant reduction of processing cycle times.

Various techniques for characterizing the dispersion of a number of layered silicates in PCL will be discussed in this paper, paying attention to their sensitivity to the different length scales and physico-chemical aspects of the nanocomposite morphology. Morphological characterization by means of atomic force microscopy, transmission electron microscopy, and wide-angle X-ray scattering is first conducted to establish a qualitative reference frame for the dispersion states achieved. Subsequently, indirect evaluation methods based on thermal analysis are applied and the results – after benchmarking against the morphological data – are directly related to a macroscopic material property, i.e., the bending stiffness of the nanocomposite. In terms of indirect methods employed, it will on the one hand be evaluated to which extent the flow behavior of the material, as assessed by dynamic rheometry, is affected by subtle changes in nanofiller dispersion. On the other hand, a recently developed thermal analysis methodology [21–25] based on modulated temperature differential scanning calorimetry (MTDSC) will be applied. The thermal characteristics of PCL nanocomposites during quasi-isothermal crystallization experiments are related to the presence of an interphase region, the nature and extent of which depends on the nanofiller type used and on its dispersion state within the PCL matrix [24,25]. The practical applicability of this method will be further demonstrated in a section of the present study dedicated to evidencing the importance of melt processing conditions, showing that the presented methodology allows differentiating between systems exhibiting subtle differences in nanofiller dispersion state.

The final part of this paper aims at demonstrating the general applicability of the developed quantification methods to other types of nanoparticle-filled polymer composites, by extending the approach developed in the framework of silicate nanocomposites to PCL filled with multi-walled carbon nanotubes (MWNTs).

2. Experimental

2.1. Materials

Poly(ε-caprolactone) was obtained from Solvay Caprolactones (presently Perstorp Caprolactones, UK) and is commercialized under the trade name CAPA®6500 (M_n = 47.500 and M_w = 84.500 g/mol according to the manufacturer).

Bentone®108 (further denoted *B108*) is a natural hectorite exchanged with dimethyl bis(hydrogenated tallowalkyl) ammonium (Elementis Specialties, USA). Nanofil®15 (abbreviated *N15*) is a natural montmorillonite exchanged with dimethyl dioctadecyl ammonium (Süd-Chemie A.G.,

Germany); Nanofil®SE3010 (further denoted *N3010*) is based on a similar compound, but its exact composition remains proprietary information of Süd-Chemie. Cloisite®10A (in short *C10A*) and Cloisite®30B (in short *C30B*) are both based on natural montmorillonite, exchanged with benzyl dimethyl tallowalkyl ammonium and methyl bis(2-hydroxyethyl) tallowalkyl ammonium, respectively (Southern Clay Products, USA). Note that the layered silicates from both the *Cloisite* and the *Nanofil* series are presently commercialized by Rockwood Specialties, Inc. (USA).

Multi-walled carbon nanotubes (MWNTs) produced by catalytic carbon vapor deposition and commercialized under the trade name Nanocyl 7000 (in short *N7000*) were supplied by Nanocyl S.A. (Belgium) and were used without further purification.

2.2. Nanocomposite preparation

The nanocomposites of this work, with filler contents up to 10 wt.%, were prepared by melt mixing at 130 °C using a batch-operated lab-scale twin-screw DSM Xplore Micro-Compounder (15 cc, N_2 purge, screw rotation speed of 170 rpm). Unless otherwise specified, the residence time within the extruder was 30 min. All compositions are expressed in terms of the inorganic filler content, as determined from thermogravimetric analysis under nitrogen (TA Instruments Q5000 TGA, 25 ml/min N_2).

Subsequent to melt mixing, all nanocomposites were compression-molded at 140 °C under 100 bar pressure using an Agila PE 30 hydraulic press.

2.3. Characterization techniques

Morphological information was obtained at room temperature from atomic force microscopy (AFM) on cryo-microtomed samples (Leica Ultracut cryo-microtome equipped with a diamond knife and maintained at −105 °C). Images were recorded in tapping-mode using an Asylum Research MFP-3D atomic force microscope equipped with an Olympus AC 240TM cantilever (resonance frequency 70 kHz, spring constant 2 N/m). Transmission electron microscopy (TEM) was conducted on cryo-microtomed slices using a Philips CM200 (120 kV acquisition voltage).

Wide-angle X-ray scattering (WAXS) was performed using a Siemens D5000 diffractometer with Cu Kα-radiation, operating at 40 kV and 40 mA.

Small angle oscillatory shear rheometry ('dynamic rheometry') experiments were performed on a TA Instruments AR-G2 rheometer fitted with a 25 mm stainless steel cone-and-plate geometry (cone angle 4°). Frequency sweep experiments were conducted at 100 °C using a strain amplitude of 0.25%, i.e., within the linear visco-elastic region as determined from strain sweep experiments at a frequency of 1 Hz.

Thermal characterization using Modulated Temperature Differential Scanning Calorimetry (MTDSC) was performed using a nitrogen-purged (25 ml/min) TA Instruments Q2000 DSC equipped with a Refrigerated Cooling System (RCS). Temperature and enthalpy calibration were performed using an indium standard; heat capacity calibration was performed using sapphire disks. The selected temperature modulation conditions during quasi-isothermal experiments were an amplitude of ±0.5 °C and a period of 60 s. Prior to measurement, all nanocomposites were dried overnight at 65 °C under vacuum. Experiments were initiated by a stay in the melt (1 h at 130 °C) in order to fully erase the thermal history of the samples.

The mechanical properties of the various materials were assessed by determining their secant modulus (3-point bending mode, 90 mm span, 4 mm deflection) at 21 °C using a Lloyd Instruments LRX Plus apparatus. An average of three measurements was taken for each sample; measurements were performed 7 days after compression molding (storage temperature 21 °C, sample dimensions $130 \times 30 \times 1.6$ mm).

To assess the electrical conductivity of carbon nanotube-based composites, 4-point conductivity measurements were directly performed on the surface of the nanocomposite films using a Keithley 6512 Programmable Electrometer (current range 1.1×10^{-6}–1.1×10^{-2} A; voltage range 10^{-4}–10^{0} V). A colloidal graphite paste provided by Electron Microscopy Science was employed to ensure proper contact between the sample and the measuring electrodes.

3. Results and discussion

A wide range of PCL/layered silicate nanocomposites was prepared by melt mixing. Care was taken to use optimized and reproducible processing conditions in order to enable the comparison of systems based on different organically modified silicates. Prior to thermal and mechanical characterization, all samples were analyzed with regard to the nanofiller dispersion state by morphological analysis to establish a reference frame for subsequent benchmarking.

3.1. Nanocomposite morphology

3.1.1. Microscopic techniques

AFM and TEM imaging allow a direct visual observation of the silicate dispersion within a polymeric matrix; however, for a reliable qualitative evaluation of the nanofiller dispersion state (exfoliated/intercalated/microcomposite), care should be taken to image truly representative areas of the sample, preferably at different magnifications.

Fig. 1a shows a tapping-mode AFM image of PCL containing 3 wt.% of *C30B* filler. Individual (flat-on) silicate platelets can be clearly observed throughout the entire matrix, attesting for a largely exfoliated nanocomposite morphology. TEM imaging confirms the occurrence of finely dispersed silicate platelets throughout the entire matrix (Fig. 1d). AFM and TEM images of a similar PCL sample filled with 3 wt.% of *B108* are shown in Fig. 1b and e, respectively. Both individual silicate platelets as well as larger aggregates can be observed by both methods, attesting for the occurrence of partially disrupted stacks of silicate platelets after processing, hence for an intercalated/exfoliated morphology. Fig. 1c and f, finally, show AFM, respectively, TEM images of a PCL sample filled with

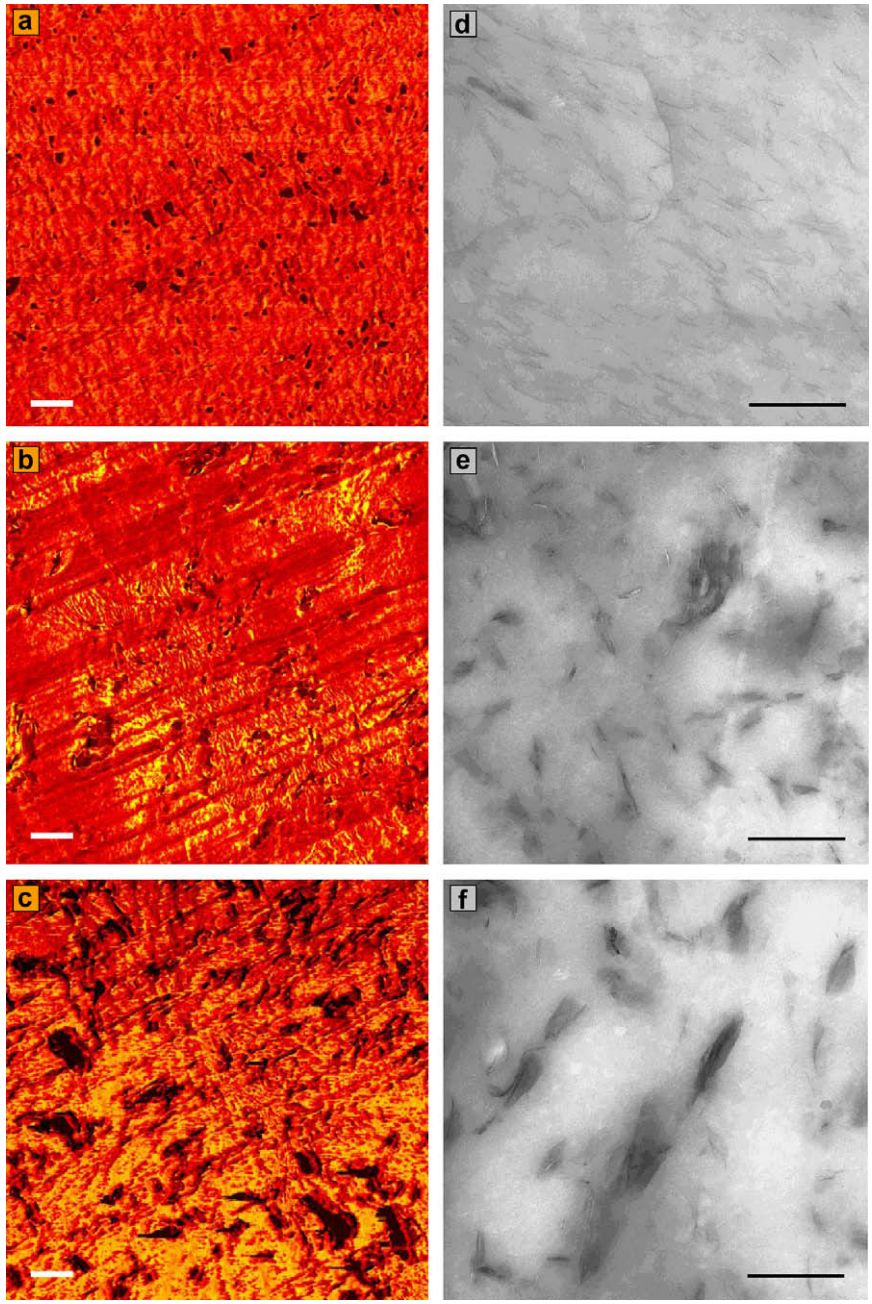

Fig. 1. Tapping-mode AFM phase images (a–c) and corresponding TEM micrographs (d–f) showing the degree of silicate dispersion in PCL nanocomposites containing 3 wt.% of Cloisite 30B (a and d), 3 wt.% of Bentone 108 (b and e), and 3 wt.% of Nanofil SE3010 (c and f); the scale bars measure 500 nm.

3 wt.% of *N3010* clay. In this case, large silicate aggregates of almost micrometer size are observed throughout the sample, which is indicative for a poor dispersion state and a morphology which is at best intercalated with large aggregates of stacked silicate layers.

3.1.2. Wide-angle X-ray scattering

As an alternative to direct visual observation, WAXS is generally employed to assess the degree of nanofiller dispersion in silicate-based nanocomposites [26]. An intercalated morphology is characterized by the occurrence of specific more or less intense scattering peaks, the position of which corresponds to the intergallery spacing within the periodically stacked silicate tactoids. Exfoliated or more disordered intercalated morphologies, on the other hand, are characterized by the complete absence of any scattering peaks in the range 2–8° 2θ. Representative examples of the information typically obtained from WAXS analysis

are shown in Fig. 2. Fig. 2a shows the WAXS profiles for a series of PCL nanocomposites as a function of *C30B* silicate loading. The absence of characteristic scattering peaks at low loading reflects an exfoliated (or disordered intercalated) morphology; upon increasing the silicate loading, a weakly intense scattering peak appears, corresponding to an intercalated morphology with an intergallery spacing of 33–34 Å. In contrast, a comparable series of PCL nanocomposites containing *N15* silicate exhibits fairly intense scattering peaks over the entire loading range (Fig. 2b), attesting for an intercalated morphology with an intergallery spacing of 32–33 Å. These results already indicate the lower extent of silicate exfoliation in nanocomposites containing non-polar silicate modifier (*N15*), whereas high dispersion degrees can be achieved with more polar modified silicates (*C30B*) [15,27]. Similar observations are obtained from WAXS data on the samples shown in Fig. 1 (not shown here), confirming the conclusions drawn above from AFM and TEM imaging. It should be stressed, however, that since WAXS provides a fingerprint of the gallery structure of the silicate, it is only able to provide a qualitative estimation of the occurrence of exfoliation. A lack of silicate reflection does not necessarily mean complete exfoliation, and disordered tactoids or agglomerates may exist even in composites having WAXS patterns without silicate reflection.

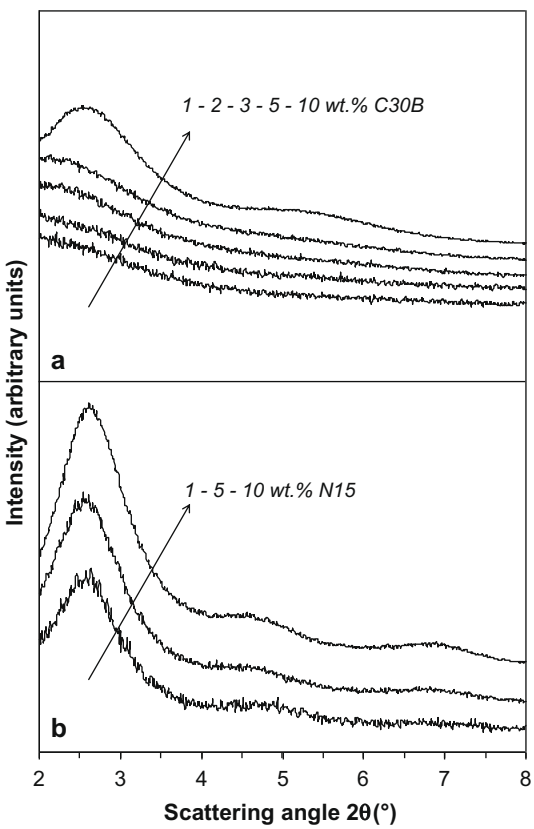

Fig. 2. Representative WAXS profiles for PCL nanocomposites containing Cloisite 30B (a) or Nanofil 15 (b) at indicated loadings (increasing in the sense of the arrows).

3.1.3. Dynamic rheometry

Frequency sweep experiments were conducted for PCL/layered silicate nanocomposites at various loadings. The occurrence of a solid-like behavior in the low-frequency region is well-established for nanocomposites containing layered silicates [28,29]. It is attributed to a retarded molecular relaxation due to the formation of a percolating network structure of filler particles [30,31], also referred to as a *house of cards* structure [32]. Fig. 3 shows the rheological response during frequency sweep experiments for a series of PCL nanocomposites at various *C30B* loadings. In the storage shear modulus, a deviation from the liquid-like terminal behavior (Fig. 3a) is clearly observed, to an extent increasing with silicate loading, attesting for the formation of a well-dispersed percolating network of filler particles. A similar behavior can be observed in the loss shear modulus, whereas the phase angle at low frequency evidences elastic behavior. This is also clearly visualized in Fig. 3b, where geometrical percolation is detected in the rheological equivalent of a so-called Cole–Cole plot [33,34] by the occurrence of a *rigid tail*, i.e., the deviation from an arc-shaped pattern when plotting the imaginary against the real part of the complex viscosity [17]. Note that geometrical percolation is already noticed at a loading as low as 0.5 wt.% *C30B*, confirming the high level of nanofiller dispersion achieved under the selected melt processing conditions.

Although the dynamic rheometry results indicate a percolating filler network at 0.5 wt.% loading, they do not exclude the remaining presence of a significant fraction of intercalated layered silicate. With increasing silicate loading, the contribution of tactoids and even aggregates to the filler network will increase. Nevertheless, the assessment by dynamic rheometry of the extent of "solid-like" behavior for the various PCL nanocomposites indirectly allows a qualitative comparison between the exfoliation states of the different organically modified layered silicates, provided that the same polymer matrix is used in all systems, that the silicate weight (or volume) fraction is kept constant, that the various nanocomposites are pre-

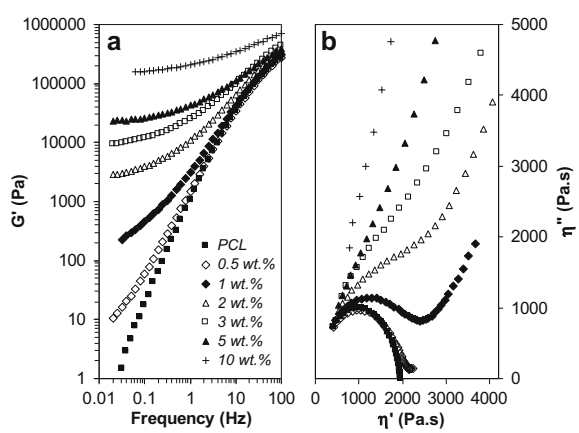

Fig. 3. Dynamic rheometry data from frequency sweep experiments on PCL and its nanocomposites at various Cloisite 30B loadings: storage shear modulus vs. frequency (a) and Cole–Cole representation (b).

pared using the same processing conditions, and that the measurements are performed under constant experimental conditions.

3.2. The effect of silicate modifier type

Earlier reports extensively emphasized on the fact that numerous competitive interactions may develop in polymer/layered silicate nanocomposites, i.e., among the various functional groups of the organic modifier (ionic groups, hydroxyl groups, aliphatic backbone), the silicate (ionic sites, surface oxygen atoms) and the polymer [35,36]. Such specific interactions, some of which may even lead to the dissolution of the organic modifier in the polymer matrix or to the occurrence of chemical reactions, will always to a large extent govern the morphology and final properties of the elaborated materials. To illustrate this, a wide range of PCL nanocomposites containing various organically modified layered silicates has been prepared by melt extrusion in order to assess the importance of the nanofiller surface characteristics and specific matrix/filler interactions in relation to nanofiller dispersion state. The mechanical properties of the various nanocomposite materials were subsequently assessed and directly related to the nanocomposite morphology. For this purpose, the degree of nanofiller dispersion was qualitatively evaluated by dynamic rheometry and the results supported by data obtained from a novel characterization methodology which is based on advanced thermal analysis.

3.2.1. Mechanical and rheological properties

The mechanical properties of the various nanocomposite systems as a function of filler loading were evaluated in 3-point bending mode. Fig. 4 shows the secant modulus of the various systems (Fig. 4a and c) in direct comparison with the dynamic rheometry data for the corresponding systems at a fixed loading of 3 wt.% (Fig. 4b and d). For all samples, an almost linear increase in the secant modulus with increasing nanofiller loading is observed. With regard to the achieved stiffness, however, it is also clear that the choice of the organic modifier determines the nanocomposite properties to a large extent: silicates bearing more polar functional groups, e.g., *C30B*, undoubtedly show a proportionally stronger increase in nanocomposite stiffness than those bearing non-polar modifier chains. Neglecting the (unlikely) effect of silicate orientation in the present series of compression-molded nanocomposites, this dependency on silicate modification is assumed to be a direct consequence of changes in the degree of nanofiller dispersion, as confirmed by the dynamic rheometry data in Fig. 4b and d. If the deviation from the arc-shaped pattern in the Cole–Cole plots, i.e., the appearance of a *rigid tail*, is taken as a measure for nanofiller dispersion, then it clearly appears that silicates bearing more polar modifier chains (*C30B*) display a far better dispersion state in PCL than modified silicates showing less affinity for the polar matrix (*N3010*). Under constant processing conditions, the intrinsic occurrence of specific matrix/filler interactions is thus the governing factor in determining the achieved dispersion quality [25], hence

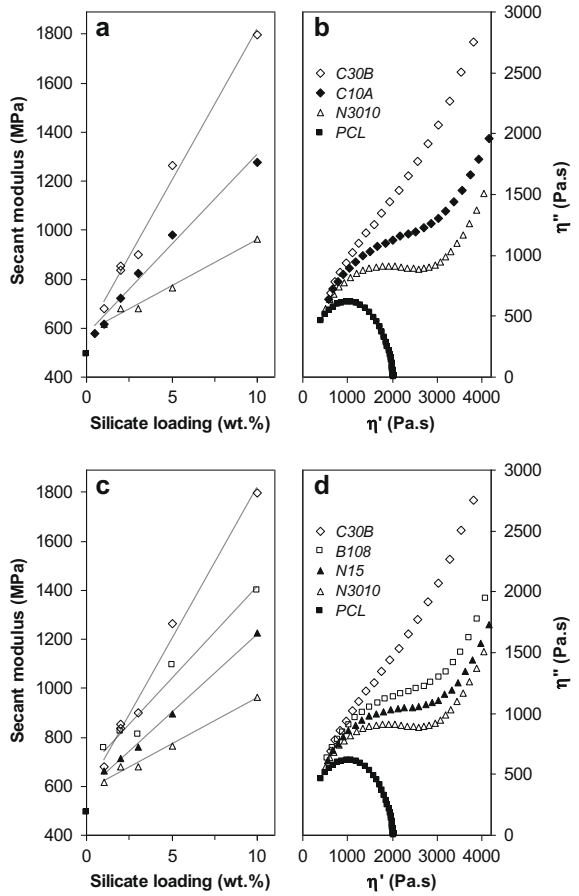

Fig. 4. Pairwise comparison of mechanical and rheological data for unfilled PCL and its nanocomposites filled with various types of layered silicates; mechanical data show the secant modulus as a function of silicate loading (a and c), whereas rheological data show the corresponding Cole–Cole plots at a fixed loading of 3 wt.% (b and d). Data for PCL filled with Cloisite 30B and Nanofil SE3010 appear on all graphs as a suitable base for comparison, i.e., best and worst dispersion quality, respectively. The solid lines are guidelines to the eye.

also the resulting stiffness improvement of the material. Determining the interaction strength between the polymer and the organically modified silicate through the reversible work of adhesion [37] or through molecular dynamics computation of the interaction energies [35,36] could support the relation between the presence of polar moieties on the silicate modifier and the resulting affinity for the PCL matrix; this is, however, judged beyond the scope of the present paper.

In the context of the above discussion it is to be mentioned that both geometrical percolation (in a rheometric experiment) and stiffness increase (in a 3-point bending test) also depend on the aspect ratio of the dispersed nanofiller particles. However, in view of the very similar particle dimensions of the various silicate fillers used, in addition to the clear trends observed within a given family of silicate fillers (e.g., compare the various Cloisite-based nanocomposites in Fig. 4), it is assumed that the characteristics of the modified filler surface do play the dominant role in the present comparison [25].

It is clear from the foregoing that dynamic rheometry is a highly valuable technique for qualitatively comparing the extent of silicate dispersion within a thermoplastic matrix. As an illustration of the differences that may exist upon using different organically modified silicates, Fig. 5 shows dynamic rheometry data for various PCL/layered silicate nanocomposites at 1 and 3 wt.% loading in a single Cole–Cole plot, evidencing the occurrence of a rigid tail to various extents. Additionally, marked differences can be observed when looking at the evolution of the phase angle δ with frequency for the various nanocomposites at 3 wt.% loading (Fig. 6a). For unfilled PCL, a low-frequency plateau value of the phase angle close to 90° is characteristic for a viscous flow behavior. For the nanocomposites, however, the low-frequency phase angle δ starts well-below 90° and increases towards a maximum at higher frequencies; the lower phase angle at low frequencies is again indicative for a solid-like flow behavior as it reflects and increasing elastic contribution to the visco-elastic response. When comparing the various layered silicates at 3 wt.% loading, it is observed that a decreasing phase angle δ at low frequency (Fig. 6) correlates well with an increasing *rigid tail* in the Cole–Cole plots (Fig. 5) and an increasing secant modulus (Fig. 4). In the established ranking, *C30B* clearly shows the highest level of solid-like behavior, which implies the highest level of filler dispersion assuming similar aspect ratios, whereas *N3010* is clearly the silicate showing the worst dispersion. As such, the rheological data facilitate establishing some guidelines as to which, out of the vast number of available organically modified silicates, has the highest affinity for PCL and is, consequently, the better suited for incorporation into a PCL matrix. *C30B*, the most polar organically modified silicate in our series as a result of the presence of hydroxyl moieties on the modifier chains, clearly has the highest affinity for PCL and leads to the highest dispersion level. *B108*, *N15* and *C10A* contain less polar alkylammonium substituents and show an intermediate affinity for the PCL matrix. Finally, *N3010*, which is recommended for non-polar matrices [38] and is therefore thought to bear a modifier with non-polar substituents, displays a lower affinity for PCL and clearly results in a poorer dispersion. It can thus be unambiguously concluded that the choice for an organically modified silicate containing more polar substituents is highly beneficial with regard to the achievable dispersion state within a PCL matrix, hence to the level of mechanical reinforcement that can be targeted.

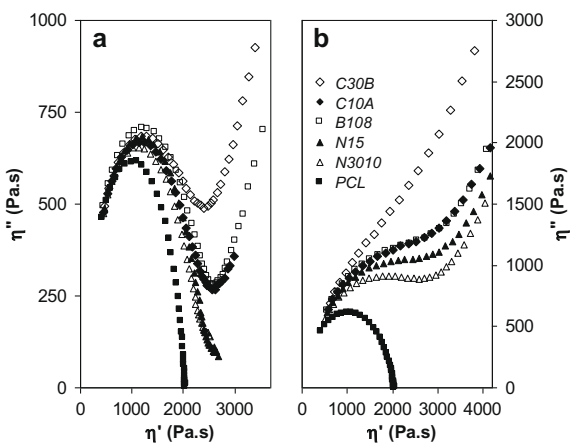

Fig. 5. Dynamic rheometry overview graph showing Cole–Cole plots for unfilled PCL and for all silicate-based nanocomposites at a loading of 1 wt.% (a) and 3 wt.% (b).

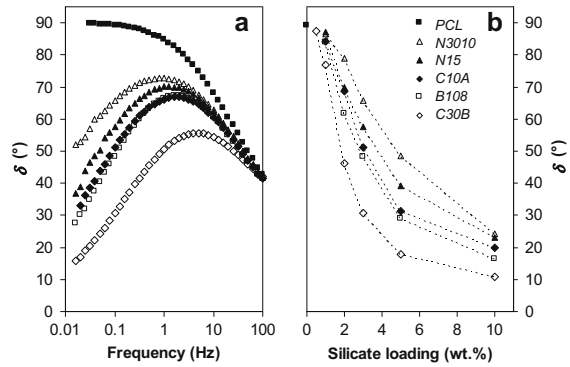

Fig. 6. Dynamic rheometry data from frequency sweep experiments on PCL and its nanocomposites containing various types of organically modified layered silicates: phase angle δ as a function of frequency for PCL and its nanocomposites at a silicate loading of 3 wt.% (a), and phase angle δ at 0.1 Hz frequency, as determined during a frequency sweep experiment, plotted against silicate loading (b).

Pertaining to the qualitatively established dispersion ranking, it is finally also worth noting that, at a relatively low loading of 1 wt.%, only the best dispersed layered silicates generate the occurrence of a marked *rigid tail* in a Cole–Cole plot (Fig. 5a) and a low-frequency phase angle below 90° (Fig. 6b), whereas the more poorly dispersed nanofillers show almost liquid-like behavior. At higher filler loading, i.e., beyond the threshold for geometrical percolation, all nanocomposite samples display more or less important solid-like behavior (Figs. 5b and 6b).

3.2.2. Thermal properties from MTDSC analysis

An advanced thermal analysis method based on modulated temperature DSC was recently introduced as a novel tool for monitoring the degree of nanofiller dispersion in a semi-crystalline polymer matrix [21–25]. This characterization method exploits the occurrence of an 'excess' heat capacity, C_p^{excess}, recorded during quasi-isothermal crystallization experiments and caused by reversible melting and crystallization phenomena on the timescale of the imposed temperature modulation. It was demonstrated that the magnitude of this 'excess' heat capacity C_p^{excess}, evaluated at steady-state conditions, can be related to the nanofiller dispersion state within a given family of nanocomposite materials [25]. Fig. 7 shows an overview graph collecting all C_p^{excess} data for the PCL nanocomposite series of this work as a function of silicate loading. It is observed that all curves level off at higher loading, despite a further increase in the mechanical properties up to the highest loadings considered in this study. This plateau reflects some extent of saturation beyond *ca.* 5 wt.% silicate loading, i.e., a situation in which the degree of nanofiller dispersion becomes limited due to the physical impossibility to further delaminate individual platelets in a highly loaded system. As a result, further

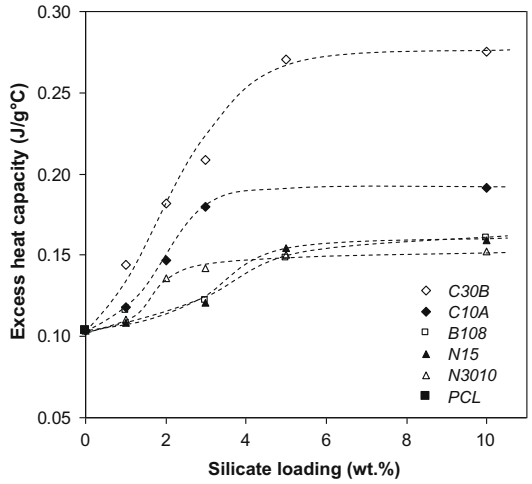

Fig. 7. MTDSC excess heat capacity C_p^{excess} recorded during quasi-isothermal crystallization experiments on unfilled PCL and its nanocomposites (50 ± 0.5 °C/60 s), as a function of silicate content; the dashed lines are guidelines to the eye.

increasing the silicate loading does not further affect the thermal properties of the material, even though it is still beneficial in terms of modulus increase (Fig. 4). When evaluated at the saturation value, the observed C_p^{excess} trends from Fig. 7 confirm the conclusions drawn from AFM and TEM observation, mechanical characterization and dynamic rheometry, with a proportionally higher magnitude of C_p^{excess} for the better dispersed silicates [39], i.e., those showing the highest affinity for the PCL matrix.

3.3. The effect of nanocomposite processing conditions

With regard to the achievable dispersion quality, matrix/filler affinity clearly is a key factor determining the outcome for any polymer/filler combination. However, proper nanocomposite melt processing can be equally crucial as delamination and true nano-scale dispersion of individual silicate platelets are only achieved under well-conceived conditions of temperature, shear and residence time [25,40–46].

In this study, PCL nanocomposites containing the organically modified layered silicate showing the highest affinity of all investigated, i.e., *C30B*, were prepared by melt extrusion using a small-scale batch extruder, focusing on the importance of residence time under maximum achievable shear intensity (245 rpm screw rotation speed). The choice for this silicate filler is dictated by the fact that it intrinsically allows the highest level of nanofiller dispersion to be achieved, as demonstrated above. The various developed methods for assessing the nanofiller dispersion state are subsequently applied to evaluate the achieved nanocomposite morphology and final properties. Note that a detailed study on the influence of additional processing conditions, such as temperature, screw speed and throughput, along with extrusion modeling results, is part of our ongoing research activities.

Fig. 8a shows the secant modulus for unfilled PCL and for samples containing 1 or 5 wt.% of *C30B* as a function of extruder residence time. The stiffness of the nanocomposite samples increases with increasing residence time up to a certain plateau level. Further increasing the residence time does not result in an additional increase in the nanocomposite stiffness. Direct visual observation from TEM imaging confirms the pronounced changes in the achieved dispersion state: whereas a large number of tactoids of stacked silicate platelets can still be clearly observed in PCL filled with 5 wt.% *C30B* after 2 min processing time, the same sample processed for 1 h unambiguously shows individually dispersed (and randomly oriented) silicate platelets throughout the entire matrix (Fig. 9). The observed trends clearly reflect a changing degree of silicate dispersion as a function of extruder residence time, emphasizing the importance of well-adjusted processing conditions.

C_p^{excess} measurements were conducted on the same series of samples in order to assess the degree of silicate dispersion in the PCL matrix as a function of processing time. In accordance with the mechanical data reported in Fig. 8a, the thermal data in Fig. 8b clearly show that, whereas the reference C_p^{excess} level for unfilled PCL remains unaffected by an increasing residence time, the filled samples do display a pronounced evolution. The observed increase in C_p^{excess} thus points at a nanofiller dispersion state steadily improving with time in the high-shear environment of the melt extruder, resulting in a continuously increasing amount of polymer/filler interface and associated alteration of the thermal properties of the PCL matrix [24,25]. Beyond a certain residence time the recorded C_p^{excess} level remains constant, indicating that a steady-state situation is attained under the selected temperature and shear flow conditions, and that prolonged processing is no longer beneficial. This steady-state level is attained earlier at low filler loading, reflecting that intercalation and subsequent platelet delamination by a peeling-off mechanism [47] are less straightforward in a highly loaded and geometrically jammed system. Note also that GPC measurements

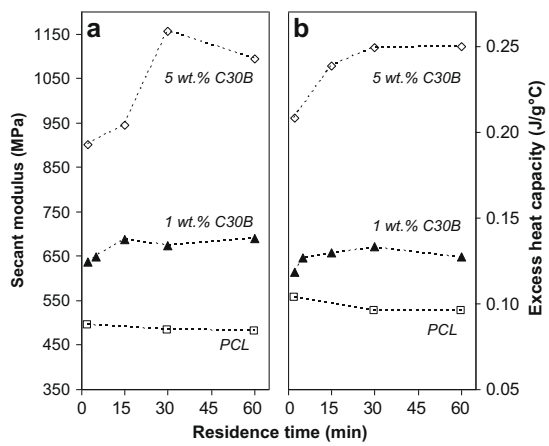

Fig. 8. Secant modulus (a) and excess heat capacity C_p^{excess} (b) for unfilled PCL and its nanocomposites containing 1 and 5 wt.% of Cloisite 30B plotted as a function of extruder residence time; the quasi-isothermal crystallization experiments were conducted at 50 °C under a temperature modulation of ±0.5 °C/60 s.

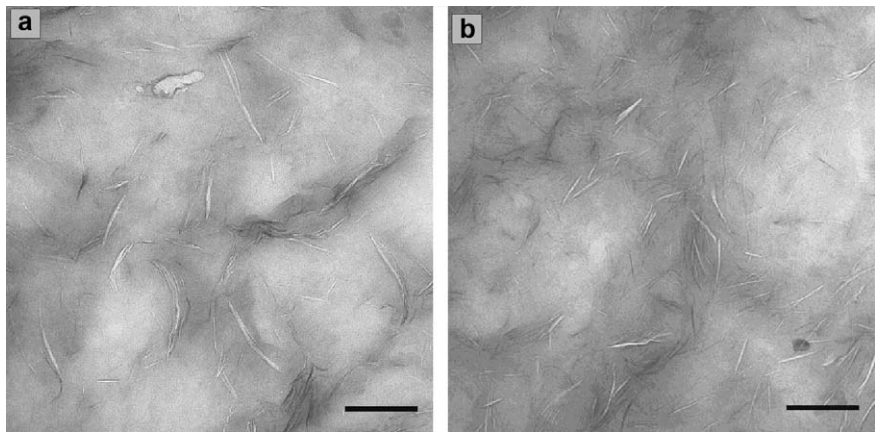

Fig. 9. TEM micrographs showing PCL nanocomposites containing 5 wt.% of Cloisite 30B and processed in a melt extruder for residence times of 2 min (a) and 1 h (b); scale bar: 200 nm.

did not reveal any significant extent of PCL matrix degradation within the range of investigated residence times.

In view of its ability to evidence subtle differences in the level of nanofiller dispersion, as reported above, dynamic rheometry was also employed to characterize the present series of samples. As an alternative to the Cole–Cole representation, Fig. 10 plots the inverse loss tangent as a function of loss modulus for unfilled PCL and for the different nanocomposite samples. This representation was demonstrated to be particularly useful for the visualization of small changes in the rheological behavior of the material inferred by the filler particles [48,49]. As anticipated, the unfilled PCL follows a nearly straight line independently of the extruder residence time (corresponding to an arc shape in a Cole–Cole plot). A clear deviation from this behavior is noticed, however, upon incorporation of layered silicates, attesting for the formation of a percolating network structure (*cf.* the *rigid tail* in the Cole–Cole representation). Moreover, a clear effect of extruder residence time is noticed for the samples containing 1 wt.% of *C30B*, with a proportionally stronger deviation from the straight line with increasing residence time. This result once more confirms that the achievement of a truly dispersed nanocomposite system requires a prolonged melt mixing time, as already noticed above. Surprisingly, however, the dynamic rheometry data do not reveal a comparable trend in the highly loaded PCL samples, despite clear indications for an increasing degree of silicate dispersion as observed from C_p^{excess} data (5 wt.% *C30B*, see Fig. 8b) and from direct visual observation on TEM micrographs (Fig. 9). This finding illustrates that, beyond a certain nanofiller loading, dynamic rheometry becomes insensitive even to fairly pronounced differences in the dispersion state of the nanocomposite samples. At higher loadings, the elastic response due to the solid-like *house of cards* structure of silicate platelets dominates the flow behavior and, unlike for C_p^{excess} measurements, dynamic rheometry no longer allows to discriminate between varying degrees of nanofiller dispersion [50]. This observation therefore also illustrates the need to use multiple characterization techniques in order to truly assess the nanocomposite dispersion state, and further demonstrates the added value of using C_p^{excess} data as a measure for nanofiller dispersion.

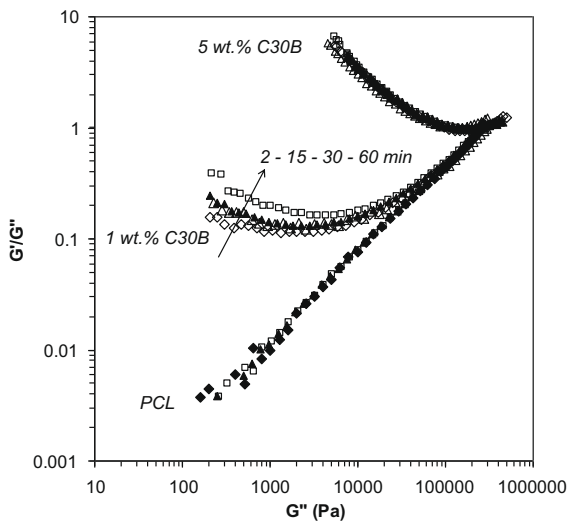

Fig. 10. Inverse loss tangent G'/G'' as a function of loss shear modulus G'' during frequency sweep experiments on unfilled PCL and its nanocomposites containing 1 and 5 wt.% of Cloisite 30B; nanocomposite processing using indicated extruder residence times (corresponding symbols are used for all three data sets).

3.4. Extension to carbon nanotube-based systems

So far, the methods for assessing the nanofiller dispersion state have been discussed in the context of layered silicate nanocomposites, showing the large potential of MTDSC and dynamic rheometry experiments. These methods are, however, not at all restricted to platelet-shaped nanoparticles. As an illustration, the developed methods were also employed for comparing the nanofiller dispersion state in nanocomposites containing carbon nanotubes.

Morphological information on the PCL/carbon nanotube composites was obtained from AFM imaging, as shown in Fig. 11. On the scale shown, individual carbon nanotubes can be clearly discerned, pointing at a high level of carbon

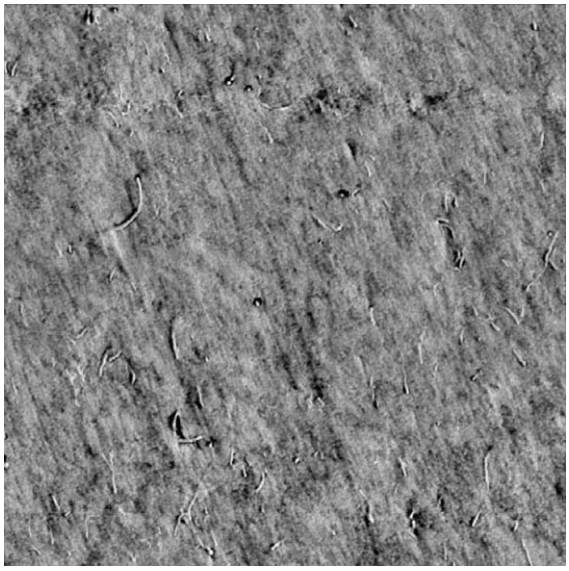

Fig. 11. Tapping-mode AFM phase image showing the degree of carbon nanotube dispersion in a PCL nanocomposite containing 3 wt.% of Nanocyl 7000; depicted area: 2.8 × 2.8 μm².

nanotube dispersion. As a result, significant improvement in the bending stiffness of the nanocomposites might be anticipated. However, as illustrated in Fig. 12a, the reinforcing effect is far more limited than with well-dispersed *C30B* layered silicate at equal loading. Moreover, in case of carbon nanotubes, the increase in secant modulus with carbon nanotube loading shows a clear deviation from a linear trend at as little as 0.5 wt.% loading, possibly attesting for an incomplete carbon nanotube individualization. Earlier results from scanning electron microscopy confirm the fairly high level of carbon nanotube dispersion evidenced by AFM, but observation on a larger scale also reveals the presence of carbon nanotube aggregates that limit the improvement in mechanical performance of the samples [24]. This effect is especially pronounced at higher loading, where carbon nanotube entanglements limit their dispersion as individual high aspect ratio particles.

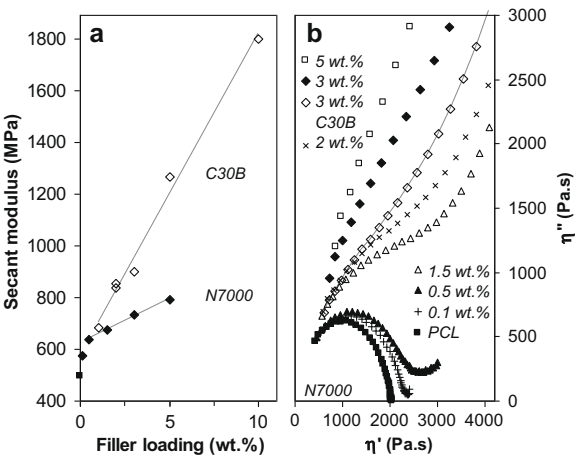

Fig. 12. Pairwise comparison of mechanical and rheological data for unfilled PCL and its nanocomposites filled with carbon nanotubes (Nanocyl 7000) as well as with layered silicates for comparison (Cloisite 30B); mechanical data show the secant modulus as a function of carbon nanotube or silicate loading (a), whereas rheological data show the corresponding Cole–Cole plots at various carbon nanotube loadings and at 3 wt.% silicate loading for comparison (b).

As in the case of layered silicate nanocomposites, dynamic rheometry is very sensitive to the presence of well-dispersed carbon nanotubes [51,52] since network formation is a common particularity of both classes of materials. Fig. 12b shows Cole–Cole plots for unfilled PCL and for nanocomposites containing various carbon nanotube (*N7000*) loadings. A marked deviation from liquid-like behavior can be observed at filler loadings beyond 0.5 wt.%; a very slight effect can even already be noticed at a loading as low as 0.1 wt.%, confirming the high degree of MWNT dispersion achieved. Earlier reports mentioned geometrical percolation in PCL nanocomposites at a carbon nanotube loading of 0.35 wt.% [19], and for melt-mixed samples even beyond 2–3 wt.% [17]. The solid-like behavior becomes progressively more pronounced at higher carbon nanotube loading, evidencing an increasingly elastic flow response accompanying the formation of a percolating network of carbon nanotubes [51,53]. For comparison, Fig. 12b also includes a Cole–Cole plot for PCL filled with 3 wt.% of *C30B* layered silicate (as marked by the solid line). It appears that, at equal loading, carbon nanotubes have a proportionally stronger effect on the rheological behavior than layered silicates. Even though a truly quantitative evaluation of the dispersion state of both fillers cannot be conducted at present and would probably evidence marked differences, the observed discrepancy in the rheological behaviors most probably originates from the significantly higher aspect ratio of the carbon nanotubes, a factor which reportedly determines geometrical (as well as electrical) percolation [54,55]. Still, as shown in Fig. 12a, carbon nanotubes display a lower reinforcing effect than well-dispersed layered silicates – despite the higher aspect ratio – as a result of their strong entanglement and the associated difficulty to achieve a proper dispersion state. Accordingly, the mechanical properties of carbon nanotube composites are frequently dominated by inter-tube slippage in nanotube bundles – especially at higher loadings – thus remaining below expectations [56].

In the particular case of carbon nanotube-based composites, electrical conductivity measurements are frequently employed to assess the filler dispersion state through the determination of an electrical percolation threshold, i.e., the nanotube loading at which filler connectivity is achieved and a marked increase is observed in the electrical conductivity [57]. The data in Fig. 13a indicate that electrical percolation is reached at a MWNT loading slightly above 0.5 wt.%. Note that Fig. 12b already indicated geometrical percolation at 0.5 wt.% loading, in line with the connection that has been advanced between electrical and rheological percolation [53].

For comparison, and in order to validate the developed modulated temperature DSC methodology in an extension to carbon nanotube-based composites, quasi-isothermal crystallization experiments were conducted for this

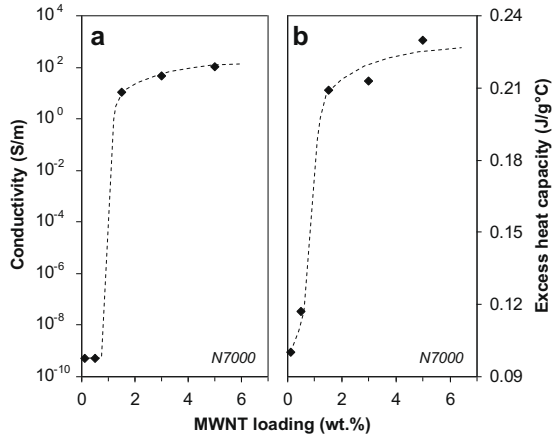

Fig. 13. Electrical conductivity (a) and excess heat capacity C_p^{excess} (b) as a function of carbon nanotube loading for PCL nanocomposites containing Nanocyl 7000; the quasi-isothermal crystallization experiments were conducted at 55.5 °C under a temperature modulation of ±0.5 °C/60 s; the dashed lines are guidelines to the eye.

particular series of MWNT-filled PCL nanocomposites. As for the previously discussed layered silicate-based nanocomposites, Fig. 13b reveals a strong dependence of C_p^{excess} on nanofiller loading, the increase in C_p^{excess} being stronger in the presence of carbon nanotubes as compared to layered silicates [24]. The observed tendency in C_p^{excess} largely parallels the trend revealed from electrical conductivity measurements (Fig. 13a), not only confirming the wide application potential of the developed thermal analysis methodology, but also illustrating that it provides a valuable alternative to the methods commonly employed for assessing nanofiller dispersion. Noteworthy, C_p^{excess} measurements even appear to be the method of choice at *low* filler loadings, where both electrical conductivity and dynamic rheometry show to be largely insensitive to changes in the nanofiller dispersion state.

4. Conclusions

Aiming at critically reviewing some of the available methods for assessing nanofiller dispersion within a polymeric matrix, the rheological, mechanical and thermal properties of melt-extruded PCL nanocomposites containing a wide range of organically modified layered silicates have been evaluated in direct relation to morphological information obtained from atomic force microscopy, transmission electron microscopy and wide-angle X-ray scattering.

It was recognized that none of the employed techniques is able provide a direct and truly quantitative assessment of the nanofiller dispersion state:

- *Dynamic rheometry* effectively indicates the formation of a percolating silicate network, but although the extent of network formation must depend on the degree of silicate exfoliation, its occurrence can definitely not be considered an unambiguous fingerprint of an exfoliated state.
- The *secant modulus* is without a doubt fairly sensitive to the extent of silicate dispersion, but as it depends on the overall structure of the nanocomposite it may be influenced by aspects such as an altered degree of crystallinity, processing-induced filler orientation, *etc.*
- The C_p^{excess} *approach* provides accurate information on the chain segment dynamics of the matrix polymer as affected by the presence of nanofillers. It can, as such, be considered a true nano-scale characterization method. The interpretation of the obtained data may, however, be rather complex as they may be influenced by morphological changes to the crystal structure, induced by the presence of dispersed nanofillers.

Nevertheless, all three can contribute to a qualitative assessment of the filler dispersion and the main factors affecting it: the intrinsic affinity between the matrix polymer and the nano-sized filler particles, as well as the choice of nanocomposite processing conditions. It was demonstrated that PCL nanocomposites containing layered silicates with a higher intrinsic affinity for the matrix polymer show a more pronounced solid-like behavior at low frequency in dynamic rheometry experiments as well as a higher excess heat capacity during quasi-isothermal crystallization of the polymer matrix. Accordingly, those nanocomposites displaying the highest dispersion levels were also found to exhibit superior improvement in mechanical properties such as stiffness.

From a direct comparison between the various methods, the innovative C_p^{excess} *approach* was evidenced to offer a valuable alternative to the commonly employed characterization tools, providing accurate data with regard to nanofiller dispersion in addition to a more fundamental insight into interphase formation and into the way the matrix polymer is affected in the vicinity of dispersed nanofiller particles. The approach was also shown to retain good sensitivity at low nanofiller loadings, where mechanical and rheological approaches were found unsuitable to reliably discriminate between slight changes in the silicate dispersion state. Finally, the wide potential of all investigated methodologies – and especially of the recently developed C_p^{excess} *approach* – for the characterization of polymeric nanocomposites in general was illustrated by an extension to carbon nanotube-based composites.

Acknowledgements

This work is supported by a research grant of the Institute for the Promotion of Innovation by Science and Technology in Flanders (IWT-Vlaanderen, project number 060440). H.E. Miltner, N. Gotzen and G. Van Assche acknowledge the Research Foundation Flanders (FWO-Vlaanderen) for financial support. The authors are grateful to T. Segato and Prof. M.-P. Delplancke (Service de Chimie Industrielle, Université Libre de Bruxelles, Belgium) for WAXS analysis and to Y. Paint (Materia Nova, Belgium) for TEM imaging. Süd-Chemie A.G., Southern Clay Products, Elementis Specialties and Nanocyl S.A. are kindly acknowledged for providing the various nanofillers used throughout this work.

References

[1] Wagener R, Reisinger TJG. A rheological method to compare the degree of exfoliation of nanocomposites. Polymer 2003;44:7513–8.

[2] Szazdi L, Abranyi A, Pukánszky Jr B, Vancso JG, Pukanszky B. Morphology characterization of PP/clay nanocomposites across the length scales of the structural architecture. Macromol Mater Eng 2006;291:858–68.

[3] Osman MA, Mittal V, Lusti HR. The aspect ratio and gas permeation in polymer-layered silicate nanocomposites. Macromol Rapid Commun 2004;25:1145–9.

[4] Fornes TD, Paul DR. Modeling properties of nylon 6/clay nanocomposites using composite theories. Polymer 2003;44:4993–5013.

[5] Bharadwaj RK, Mehrabi AR, Hamilton C, Trujillo C, Murga M, Fan R, et al. Structure-property relationships in cross-linked polyester-clay nanocomposites. Polymer 2002;43:3699–705.

[6] Serrano MC, Pagani R, Vallet-Regi M, Pena J, Ramila A, Izquierdo I, et al. In vitro biocompatibility assessment of poly(epsilon-caprolactone) films using L929 mouse fibroblasts. Biomaterials 2004;25:5603–11.

[7] Rizzi SC, Heath DT, Coombes AGA, Bock N, Textor M, Downes S. Biodegradable polymer/hydroxyapatite composites: surface analysis and initial attachment of human osteoblasts. J Biomed Mater Res 2001;55:475–86.

[8] Bogdanov B. Isometric crystallization of stretched poly(epsilon-caprolactone) sheets for medical applications. J Therm Anal Calorim 2003;72:667–74.

[9] Alexandre M, Dubois P. Polymer-layered silicate nanocomposites: preparation, properties and uses of a new class of materials. Mat Sci Eng R 2000;28:1–63.

[10] Ray SS, Okamoto M. Polymer/layered silicate nanocomposites: a review from preparation to processing. Prog Polym Sci 2003;28:1539–641.

[11] Thostenson ETL, Chou T-W. Nanocomposites in context. Compos Sci Technol 2005;65:491–516.

[12] Schwab JJ, Lichtenhan JD. Polyhedral oligomeric silsesquioxane (POSS)-based polymers. Appl Organomet Chem 1998;12:707–13.

[13] Yang KK, Wang XL, Wang YZ. Progress in nanocomposite of biodegradable polymer. J Ind Eng Chem 2007;13:485–500.

[14] Gorrasi G, Tortora M, Vittoria V, Pollet E, Alexandre M, Dubois P. Physical properties of poly(epsilon-caprolactone) layered silicate nanocomposites prepared by controlled grafting polymerization. J Polym Sci B Polym Phys 2004;42:1466–75.

[15] Lepoittevin B, Devalckenaere M, Pantoustier N, Alexandre M, Kubies D, Calberg C, et al. Poly(epsilon-caprolactone)/clay nanocomposites prepared by melt intercalation: mechanical, thermal and rheological properties. Polymer 2002;43:4017–23.

[16] Lepoittevin B, Pantoustier N, Devalckenaere M, Alexandre M, Kubies D, Calberg C, et al. Poly(epsilon-caprolactone)/clay nanocomposites by in-situ intercalative polymerization catalyzed by dibutyltin dimethoxide. Macromolecules 2002;35:8385–90.

[17] Wu D, Wu L, Sun Y, Zhang M. Rheological properties and crystallization behavior of multi-walled carbon nanotube/poly(epsilon-caprolactone) composites. J Polym Sci B Polym Phys 2007;45:3137–47.

[18] Wu TM, Chen EC. Crystallization behavior of poly(epsilon-caprolactone)/multiwalled carbon nanotube composites. J Polym Sci B Polym Phys 2006;44:598–606.

[19] Mitchell CA, Krishnamoorti R. Non-isothermal crystallization of in situ polymerized poly(epsilon-caprolactone) functionalized-SWNT nanocomposites. Polymer 2005;46:8796–804.

[20] Haggenmueller R, Guthy C, Lukes JR, Fischer JE, Winey KI. Single wall carbon nanotube/polyethylene nanocomposites: thermal and electrical conductivity. Macromolecules 2007;40:2417–21.

[21] Miltner HE, Rahier H, Pozsgay A, Pukánszky B, Van Mele B. Experimental evidence for reduced chain segment mobility in poly(amide)-6/clay nanocomposites. Compos Interface 2005;12:787–803.

[22] Miltner HE, Van Assche G, Pozsgay A, Pukánszky B, Van Mele B. Restricted chain segment mobility in poly(amide) 6/clay nanocomposites evidenced by quasi-isothermal crystallization. Polymer 2006;47:826–35.

[23] Miltner HE, Peeterbroeck S, Viville P, Dubois P, Van Mele B. Interfacial interaction in EVA-carbon nanotube and EVA-clay nanocomposites. J Polym Sci B Polym Phys 2007;45:1291–302.

[24] Miltner HE, Watzeels N, Gotzen N-A, Goffin A-L, Duquesne E, Benali S, et al. The effect of nano-sized filler particles on the crystallization behavior, interphase formation and thermal properties in melt-blended polyester nanocomposites, submitted for publication.

[25] Miltner HE, Watzeels N, Goffin A-L, Duquesne E, Benali S, Dubois P, et al. Quantifying the degree of nanofiller dispersion by advanced thermal analysis: application to polyester nanocomposites prepared by various elaboration methods, submitted for publication.

[26] Morgan AB, Gilman JW. Characterization of polymer-layered silicate (clay) nanocomposites by transmission electron microscopy and X-ray diffraction: a comparative study. J Appl Polym Sci 2003;87:1329–38.

[27] Di YW, Iannace S, Di Maio E, Nicolais L. Nanocomposites by melt intercalation based on polycaprolactone and organoclay. J Polym Sci B Polym Phys 2003;41:670–8.

[28] Krishnamoorti R, Giannelis EP. Rheology of end-tethered polymer layered silicate nanocomposites. Macromolecules 1997;30:4097–102.

[29] Zhao J, Morgan AB, Harris JD. Rheological characterization of polystyrene-clay nanocomposites to compare the degree of exfoliation and dispersion. Polymer 2005;46:8641–60.

[30] Riva A, Zanetti M, Braglia M, Camino G, Falqui L. Thermal degradation and rheological behaviour of EVA/montmorillonite nanocomposites. Polym Degrad Stab 2002;77:299–304.

[31] Lim YT, Park OO. Rheological evidence for the microstructure of intercalated polymer/layered silicate nanocomposites. Macromol Rapid Commun 2000;21:231–5.

[32] Okamoto M, Nam PH, Maiti P, Kotaka T, Hasegawa N, Usuki A. A house of cards structure in polypropylene/clay nanocomposites under elongational flow. Nano Lett 2001;1:295–8.

[33] Cole KS, Cole RH. Dispersion and absorption in dielectrics. J Chem Phys 1941;9:341–51.

[34] Garcia-Franco CA, Mead DW. Rheological and molecular characterization of linear backbone flexible polymers with the Cole–Cole model relaxation spectrum. Rheol Acta 1999;38:34–47.

[35] Sikdar D, Katti DR, Katti KS, Bhowmik R. Insight into molecular interactions between constituents in polymer clay nanocomposites. Polymer 2006;47:5196–205.

[36] Katti KS, Sikdar D, Katti DR, Ghosh P, Verma D. Molecular interactions in intercalated organically modified clay and clay-polycaprolactam nanocomposites: experiments and modeling. Polymer 2006;47:403–14.

[37] Demjen Z, Pukánszky B, Nagy J. Evaluation of interfacial interaction in polypropylene surface treated $CaCO_3$ composites. Composites Part A 1998;29:323–9.

[38] Süd-Chemie A.G. Personal communication.

[39] Note that the qualitative agreement with the trends from dynamic rheometry is not fully retained. When evaluating C_p^{excess} at 3 wt.% loading – the loading used for dynamic rheometry analysis (Fig. 5) – a higher magnitude of C_p^{excess} is observed for *N3010* than for *B108* or *N15*, even though both rheometry and mechanical testing suggest that *N3010* is significantly less well-dispersed within the PCL matrix. This discrepancy is tentatively attributed to the presence of an additional modifier compound – next to an alkylammonium modifier – in the latter silicate type (with a total organic content of *ca.* 41 wt.% as compared to *ca.* 35 wt.% for the other organically modified silicates in this study) [38]. As non-isothermal DSC experiments on *N3010* powder reveal that these organic compounds are molten at the temperature chosen for evaluating C_p^{excess}, it is very plausible that the liquid modifier fraction may locally increase the segmental mobility of intercalated PCL chains. This *increased* chain segment mobility would indeed result in an increased magnitude of C_p^{excess}, in accordance with earlier results for poly(amide)-6 nanocomposites displaying a mobility *reduction* [21,22].

[40] Vaia RA, Jandt KD, Kramer EJ, Giannelis EP. Kinetics of polymer melt intercalation. Macromolecules 1995;28:8080–5.

[41] Hu GH, Feng LF. Extruder processing for nanoblends and nanocomposites. Macromol Symp 2003;195:303–8.

[42] Yang K, Ozisik R. Effects of processing parameters on the preparation of nylon 6 nanocomposites. Polymer 2006;47:2849–55.

[43] Wang K, Liang S, Du RN, Zhang Q, Fu Q. The interplay of thermodynamics and shear on the dispersion of polymer nanocomposites. Polymer 2004;45:7953–60.

[44] Gilman JW, Bourbigot S, Shields JR, Nyden M, Kashiwagi T, Davis RD, et al. High throughput methods for polymer nanocomposites research: Extrusion, NMR characterization and flammability property screening. J Mater Sci 2003;38:4451–60.

[45] Wang H, Zeng CC, Elkovitch M, Lee LJ, Koelling KW. Processing and properties of polymeric nano-composites. Polym Eng Sci 2001;41:2036–46.

[46] Dennis HR, Hunter DL, Chang D, Kim S, White JL, Cho JW, et al. Effect of melt processing conditions on the extent of exfoliation in organoclay-based nanocomposites. Polymer 2001;42:9513–22.
[47] Fornes TD, Yoon PJ, Keskkula H, Paul DR. Nylon 6 nanocomposites: the effect of matrix molecular weight. Polymer 2001;42:9929–40.
[48] Sepehr M, Utracki LA, Zheng XX, Wilkie CA. Polystyrenes with macro-intercalated organoclay. Part II. Rheology and mechanical performance. Polymer 2005;46:11569–81.
[49] Utracki LA, Lyngaae-Jorgensen J. Dynamic melt flow of nanocomposites based on poly-epsilon-caprolactam. Rheol Acta 2002;41:394–407.
[50] Treece MA, Zhang W, Moffitt RD, Oberhauser JP. Twin-screw extrusion of polypropylene-clay nanocomposites: Influence of masterbatch processing, screw rotation mode, and sequence. Polym Eng Sci 2007;47:898–911.
[51] Pötschke P, Fornes TD, Paul DR. Rheological behavior of multiwalled carbon nanotube/polycarbonate composites. Polymer 2002;43: 3247–55.
[52] Du FM, Scogna RC, Zhou W, Brand S, Fischer JE, Winey KI. Nanotube networks in polymer nanocomposites: rheology and electrical conductivity. Macromolecules 2004;37:9048–55.
[53] Kharchenko SB, Douglas JF, Obrzut J, Grulke EA, Migler KB. Flow-induced properties of nanotube-filled polymer materials. Nat Mater 2004;3:564–8.
[54] Celzard A, McRae E, Deleuze C, Dufort M, Furdin G, Mareche JF. Critical concentration in percolating systems containing a high-aspect-ratio filler. Phys Rev B 1996;53:6209–14.
[55] Munson-McGee SH. Estimation of the critical concentration in an anisotropic percolation network. Phys Rev B 1991;43:3331–6.
[56] Coleman JN, Khan U, Gun'ko YK. Mechanical reinforcement of polymers using carbon nanotubes. Adv Mater 2006;18: 689–706.
[57] Grossiord N, Miltner HE, Loos J, Meuldijk J, Van Mele B, Koning CE. On the crucial role of wetting in the preparation of conductive polystyrene-carbon nanotube composites. Chem Mater 2007;19: 3787–93.